The Sea Surface Bounce Channel: Bubble-Mediated Energy Loss and Time/Angle Spreading

Peter H. Dahl

Applied Physics Laboratory, University of Washington
1013 NE 40th St., Seattle, WA 98105-6698, USA

Abstract. A model is presented for the energy loss in the sea surface forward bounce channel due to attenuation from wind-speed-dependent bubbles; the model is compared to data from ASIAEX and other archival data sets. At high wind speeds the model predicts an energy loss bound, i.e., no further attenuation with increasing wind speed. Prior to reaching this bound and while there is attenuation, time and angle spreading in the forward bounce path remain largely controlled by the spectral properties of the air-sea interface, i.e., they remain unchanged by the bubbles. Once bounding of energy loss occurs, initiated by the dominance of bubble scattering over air-sea interface scattering, time and angle spreading of the arrival change profoundly.

INTRODUCTION

The process of sound energy arriving via the sea surface forward bounce path, or channel, is loosely classified using the parameter $c = 2kH\sin\theta_g$, where k is acoustic wavenumber, H is rms waveheight, and θ_g is the nominal grazing angle corresponding to specular reflection. Reflection is either important or dominant when c is less than about 1.5, and scattering dominates when c is larger than 1.5. For natural sea surfaces and typical conditions, a transition from a coherent reflection to an incoherent scattering process occurs for frequencies between about 1 and 10 kHz.

Thus, forward scattering is operative for frequencies of order 10 kHz and above but also at lower frequencies given sufficiently large kH; here, the coherent intensity loss is typically very large and intensity is for the most part incoherent. In this large-c regime an overall reduction in received incoherent intensity can also happen owing to angular spreading (and time spreading) beyond that which can be measured by the receive aperture (or processing time window), or from use of highly directional sources. Yet in some propagation modeling schemes, losses associated with coherent intensity reduction, or with time and angle spreading of incoherent intensity, have the potential of being mistaken for real energy losses. In contrast, for beam widths and receive time windows sufficiently large to capture this time and angular spreading, a zero-decibel energy loss for sound arriving via the sea surface bounce path can be readily observed in field data (in a transmission ensemble-averaged sense). For example, this has been shown in measurements taken in the O(10)-kHz frequency

range [1] and measurements taken between 400 Hz and 1500 Hz [2], but under waveheight conditions such that c spanned the range O(1-10).

For air-sea conditions that generate sufficiently high concentrations of near-surface bubbles (often requiring wind speeds in excess of 5 m/s) a true energy loss has been observed in surface duct [3] and shallow water [4] propagation measurements at frequencies in the O(1-10)-kHz range. This loss is the result of attenuation from near-surface bubbles. In this paper a model for energy loss in forward scattering from the sea surface due to such attenuation is introduced and compared to recent field measurements from the East China Sea and other archival data. The model and field data reveal that bubbles impact forward scattering from the sea surface in three phases. The first occurs under mild conditions (wind speed less than 5 to 7 m/s); here the pulse forward scattered from the sea surface is extended in time, but only at levels some 30 dB below the peak level, which itself is not attenuated. The second occurs under more vigorous conditions (wind speed 7 to 12 m/s); here a significant energy loss is observed, but time and angle spreading (dominated by rough surface scattering) remain relatively unchanged. The third occurs under still more vigorous conditions (wind speed greater than 12 to 15 m/s). Here, there is near total occlusion of the sea surface, time and angle spreading are manifestly altered, and bubble-mediated energy loss becomes bounded by scattering from bubbles.

ENERGY CONSERVATION IN FORWARD SCATTERING AND MODEL FOR ENERGY LOSS DUE TO BUBBLES

Figure 1 shows the basic geometry for forward scattering from the sea surface for an acoustic source at position P_1 and receiver at position P_2. Scattering is described by the distribution of the bistatic cross-section over the sea surface as a function of position s, with position s_{SP} corresponding to the specular point. These positions are taken to be on the plane associated with the mean sea surface height. The bistatic cross section associated with sea surface roughness $\sigma_r(s)$ is a function of frequency, geometry (source depth, receiver depth, and range), and environment (sea-surface roughness correlation function and c). We construct $\sigma_r(s)$ using a combination of surface wave measurements and modeling [1, 5].

The property of energy conservation is assumed to apply as:

$$\iint \frac{\sigma_r(s) B(s)\, dA_s}{(P_1 s)^2 (P_2 s)^2} = \frac{1}{[(P_1 s_{SP}) + (P_2 s_{SP})]^2}, \tag{1}$$

where $B(s)$ is the combined transmit and receive beam pattern weighting, and the integral on the left side over the area of sea surface is computed as a Riemann sum with area interval dA_S. This equality holds for transmit and receive beam patterns

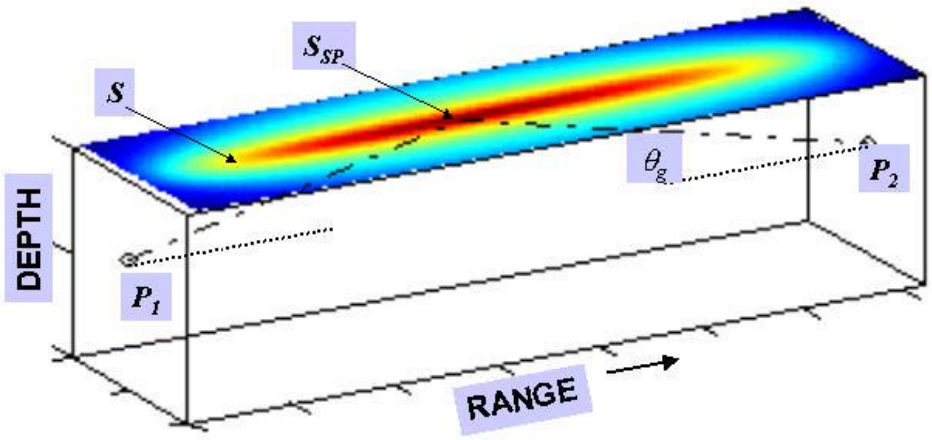

FIGURE 1. Geometry for study of forward scattering from the sea surface; source is at P_1, receiver at P_2, S_{SP} is specular point on the plane corresponding to mean sea surface and S is arbitrary point, with variable shading depicting the hypothetical sea surface bistatic cross section. Path connecting P_1, S_{SP}, and P_2 has grazing angle θ_g.

sufficiently wide to both illuminate the sea surface and receive scattered intensity from areas away from the specular point [6]. As a rough guideline [5] the necessary horizontal angular width for the case of equal source and receiver depths goes as $S_L \sin q_g$ and the vertical angular width goes as $S_L \cos q_g$, where S_L is the root-mean-square large-scale slope of the sea surface [7]. Taking S_L ~0.15 as a nominal value, the necessary one-way intensity beam width for transmit and receive is ~20°. For a more general conditions we take the left side of Eq. (1) as the energy conservation measure to be used subsequently.

Scattering and attenuation from subsurface bubbles contributes to, and modifies, the total bistatic cross section s as: $s = s_r a_b + s_b$, where a_b (dimensionless) is an attenuation factor and s_b is the bistatic scattering cross section per unit area sea surface due to bubbles [1]. Both a_b and s_b depend on the dimensionless parameter b_I, equal to the depth-integrated extinction cross section per unit volume, with b_I entering into a_b as:

$$a_b = \exp(-b_I / \sin q_i - b_I / \sin q_s), \tag{2}$$

where q_i and q_s are incident and scattered grazing angles, respectively.

The parameter b_I succinctly describes an acoustically relevant measure of the concentration of near-surface (wind-generated) bubbles; however, an expression for b_I as function of environmental conditions must necessarily be determined empirically. One such expression derived from low-angle backscattering measurements made in the O(10–100) kHz frequency range, that are exceedingly sensitive to the concentration of near-surface bubbles, is:

$$\log_{10} b_I = -6.45 + 0.47 U_{10} + 0.85 \log_{10} f, \tag{3}$$

where U_{10} is 10-m height wind speed in m/s and f is frequency in kHz [8].

The above concepts lead to a model for bubble-mediated energy loss in high-frequency ($c >> 1$) forward scattering from the sea surface, which is the following ratio expressed in dB:

$$\frac{\iint \frac{s_r(s)a_b(s)B(s)dA_s}{(P_1 s)^2(P_2 s)^2} + \iint \frac{s_b(s)B(s)dA_s}{(P_1 s)^2(P_2 s)^2}}{\iint \frac{s_r(s)B(s)dA_s}{(P_1 s)^2(P_2 s)^2}}. \qquad (4)$$

In the numerator, the left-hand (attenuation) term determines energy loss as a function wind speed (i.e., bubble concentration), and this term dominates at low to moderate wind speeds; in the absence of bubbles $a_b \to 1, s_b \to 0$, and the ratio goes to unity. At high wind speeds, the left-hand term vanishes and the right-hand (scattering) term becomes significant and establishes an *energy loss bound.* This bound is inherently a result of scattering from a two-dimensional surface. When the energy loss reaches the bound determined by bubble scattering, there is in effect total occlusion of the sea surface.

In regards to the attenuation term, we note that $a_b(s) \approx a_b(s_{SP})$, and thus Eq.(4) behaves very nearly as Eq. (2) evaluated at q_i and q_s, both set equal to the specular grazing angle q_g, with implication that energy loss scales with the inverse of q_g. A typical value for b_I is ~ 0.1 for wind speeds of 8–10 m/s and frequencies near 20 kHz; setting q_g to 10° puts a_b = 0.32, or an energy loss of about 5 dB per interaction with the sea surface. It is important to keep in mind that because the model applies only to the $c >> 1$ regime, surface decoupling (Lloyds mirror) effects [3, 9] are not operative. For the same example, when the wind speed exceeds about 12 m/s, $b_I \sim$ O(1), and the left side of the numerator in Eq.(4) vanishes. Given sufficiently wide beam patterns (as per above), the energy loss bound is 17 dB, with narrower beams resulting in a higher bound.

FIELD MEAUREMENTS FROM ASIAEX AND EARLIER STUDIES

Measurements of forward scattering from the sea surface were made in the East China Sea as part of the ASIAEX field program [5]. Figure 2 shows the sound speed profile and corresponding ray diagrams for two sets of measurements made simultaneously at frequency 20 kHz. The wind speed during these measurements (0700–0730 UTC 31 May 2001) was 7 m/s ± 0.5 m/s and the rms sea surface waveheight was 0.3 m ± 0.1 m. Based on the sound speed profile (Fig. 2a) the grazing angle associated with the specular path (dashed lines in Fig. 2) for the upper (b) and lower (c) receivers is 6.1° and 10.9°, respectively. Figure 3 shows received multi-path arrival structure for the mean intensity (based on an ensemble average of 20 transmissions) for the 26-m (upper plot) and 52-m (lower plot) receiver depths and model curves corresponding to

the mean intensity for the sea surface bounce path. (The overlap between the direct and surface bounce paths for the upper receiver is not addressed by these model curves.) Note that for modeling purposes both the source and receiver are effectively omni-directional. (There were in fact four such receivers separated by 13 cm, 30 cm, and 60 cm at each receive depth to measure vertical spatial coherence [5].)

The model curves are the result of convolving a model for the intensity impulse response [7] with the envelope of the transmit pulse (a 3-ms length boxcar function). The intensity impulse response is set by bistatic cross section s . The solid curves are based on $s = s_r$ for which an estimate of the 2-D autocorrelation function of sea surface waveheight variation is required (see [5] for additional details on this function), and the dashed curves incorporate bubbles via $s = s_r a_b + s_b$, for which a wind speed of 7.4 m/s is used, putting b_I = 0.01. Clearly, incorporating bubbles via a_b, s_b as a uniform distribution over the sea surface is a very simplified representation of the distribution of near-surface bubbles. Yet the two dashed model curves reproduce well bubble scattering phenomena observed fully 20 to 30 dB below peak scattering level and a few dB above the noise. (Model curves are made consistent with the data by adding noise, the level of which is shown in Fig. 3.) Attenuation from bubbles results in a predicted energy loss of 1.14 dB for the shallow receiver and 0.77 dB for the deep receiver; the difference is due to the different nominal grazing angles. The data are consistent with these loss estimates; however, the small difference between the two losses is difficult to verify statistically based on 20 pings.

An estimate of the time spread in forward scattering from the sea surface is made by forming the *time-delay scattering function*, which is a scaled version of the intensity impulse function. Integral measures of the time spread, defined as the characteristic time spread *L* [7], are noted in Fig. 3 for the cases with and without bubbles; they show that although the pulse extension due to bubbles (seen best with the upper receiver in Fig. 3) appears significant, the overall change in characteristic

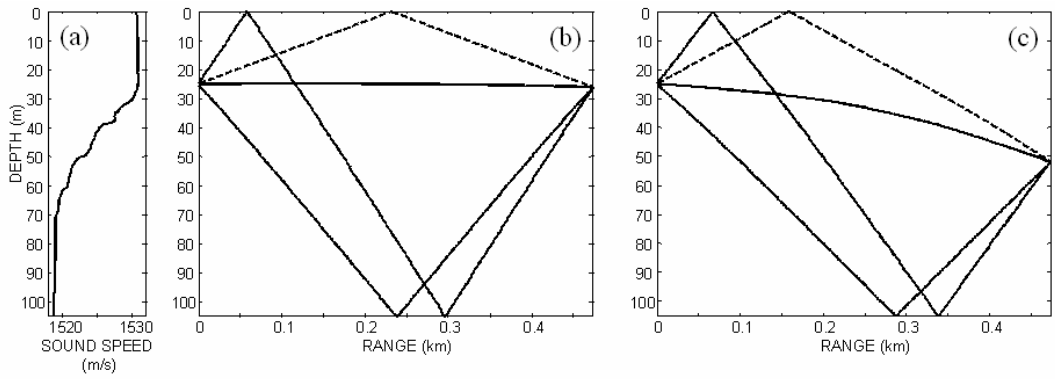

FIGURE 2. (a) Average sound-speed profile corresponding to time of acoustic measurements taken during ASIAEX, East China Sea (b) Ray diagram for 26-m depth receiver and (c) for 52-m depth receiver. Dashed lines in (b) and (c) show rays interacting once with the sea surface.

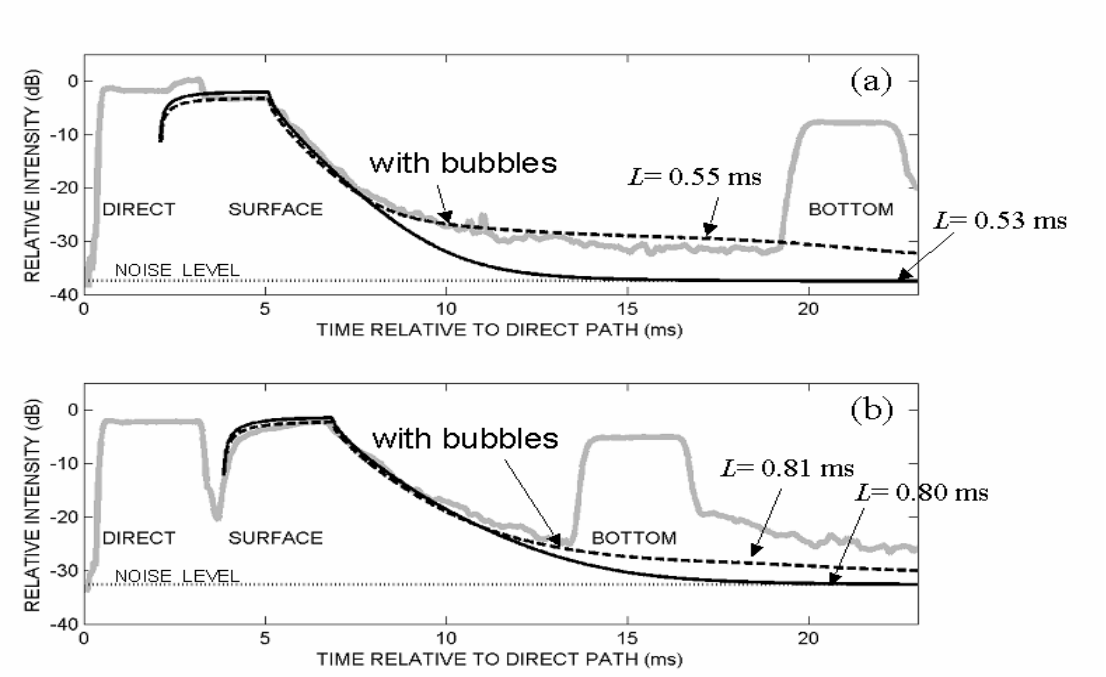

FIGURE 3. (a) Averaged received intensity (gray line) in dB plotted on relative scale (0 dB corresponds to approximately 126 dB re μPa) for the direct, surface-bounce, and bottom-bounce paths corresponding to the geometry in Fig. 2b. Solid, black line is model for mean intensity in the surface bounce path based on a 3-ms length, CW pulse with center frequency 20 kHz. Dashed, black line is same model but includes the effects of bubbles; (b) corresponds to geometry in Fig. 2c. The noise level for each geometry is shown by the dotted, black line.

time spread due to bubbles is small. There is, however, a significant difference in L associated with the different receiver depths, and a model for L [7] predicts results in Fig. 3 reasonably well, giving L = 0.67 ms and 0.83 ms for the upper and lower geometries, respectively.

A somewhat analogous, yet different, situation exists for angular spreading in the sea surface bounce path. In ASIAEX, angular spreading was determined via measurements of vertical spatial coherence [5]. The ($e^{-1/2}$) vertical coherence length d^* at 20 kHz for the 1-m VLA at the 26-m depth is 3.4 wavelengths, whereas this value is 4.0 wavelengths for the VLA located at 52 m. Angular spreading goes as $1/kd^*$, thus vertical angular spreading for the upper receiver is slightly greater than that for the lower receiver. This result is opposite that for time spreading, but consistent with the models for the geometric dependence for both time and angle spreading given in [7]. The analogy is that bubbles also have little influence on angular spreading. Spatial coherence estimates can be modeled well using an approach involving the bistatic cross section and the van Cittert-Zernike theorem [5]. Model results with and without bubbles show no difference, consistent with time and angle spreading in the sea surface bounce path being largely set by properties of rough surface scattering. Measurements made at 30 kHz displaying more substantial loss (3 dB) also suggest that characteristic time and angle spreading in forward scattering from the sea surface are altered little due to scattering from bubbles [7]. We show

subsequently that this conclusion changes when bubble concentration is sufficiently high such that total occlusion of the sea surface is in effect.

Figure 4 shows estimates of energy loss due to attenuation from near-surface bubbles (i.e., in excess of spreading and sea-water absorption) for the entire ASIAEX measurement set taken at 20 kHz and similar archived data. The ASIAEX measurements, taken over two continuous 24-h periods (separated by 6 days), represent the largest data set of this kind. There is considerable geographic variety represented in Fig. 4: ASIAEX measurements were taken in the western Pacific littoral; FLIP measurements [7] were taken in the Pacific pelagic zone; Quinault measurements [10] were taken in eastern Pacific littoral; and Whidbey measurements [11] were taken in inland waters of Puget Sound although with an extended fetch to the west. Each measurement represents a careful accounting of losses due to spreading and sea water absorption, for a single interaction with the sea surface. The error bars (not available for the data from [11]) take into account both calibration uncertainty and statistical fluctuations (giving a negative loss in some instances) that depend on the number of transmissions; e.g., uncertainty in the ASIAEX estimates is due largely to the 20 transmissions that enter into the average.

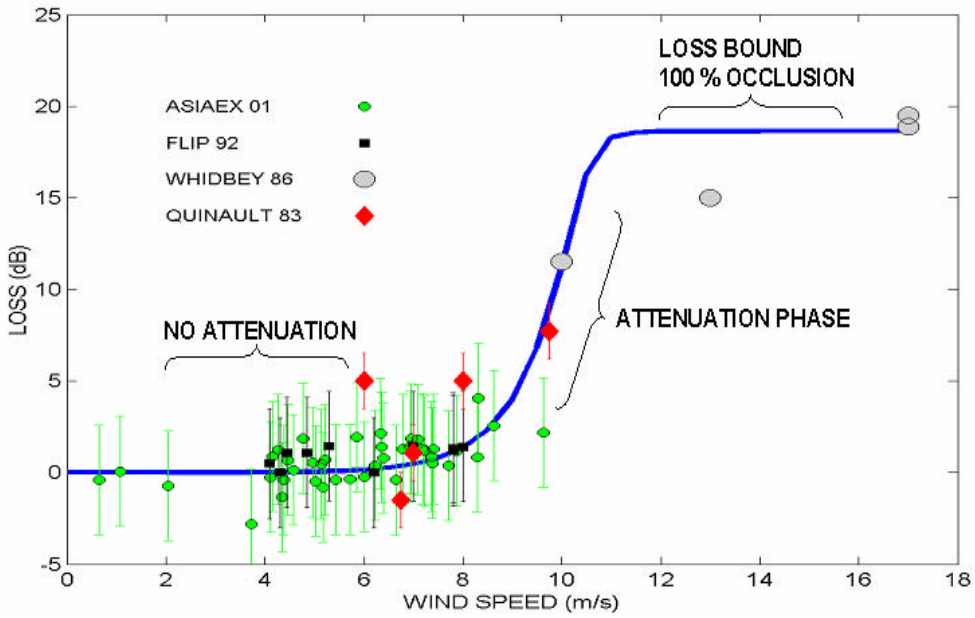

FIGURE 4. Estimates of energy loss in the single surface bounce channel due to attenuation from near-surface bubbles as a function of wind speed. Frequency is 20 kHz and nominal grazing angle is 9°. Results from four experiments (year of experiment identified in legend) are shown. Whidbey measurements were taken between 15 kHz and 25 kHz; see text for further explanation on the grazing-angle-scaling of some of these data points.

The solid curve is the bubble energy loss model based on Eqs. (3) and (4) computed at 20 kHz, with source, receiver, and range geometry such that nominal grazing angle q_g equals 9°, corresponding to the majority of the ASIAEX data; further $B(s) = 1$ because all measurements in Fig. 4 were made with omni-directional sources and receivers. Note, however, that some measurements from the other experiments were taken at grazing angles different from 9°, e.g., the FLIP measurements represent the

range q_g = 4.5–14.5°. Therefore, these data have been scaled by the factor $\sin q_g / \sin 9°$ where q_g is the particular grazing angle of the measurements.

The data and model suggest three phases of impact of bubbles on forward scattering from the sea surface: no attenuation, increasing attenuation with increasing wind speed, and an attenuation bound phase (occlusion) at very high wind speeds. Significantly, the data in Fig. 4 also demonstrate that it is very difficult to observe a loss-versus-wind-speed signature in the field measurements of forward scattering until the wind speed exceeds about 7 m/s. This contrasts with low-angle backscattering, which is exceedingly sensitive to wind speed [8], but is also consistent with the model given here, that puts the loss at only 0.45 dB at 7 m/s wind speed. With addition of the larger set of ASIAEX measurements, a transition to the attenuation phase (wind speeds between 6 m/s and 8 m/s) now appears to be displayed by the combined data set. Although the combined data set in Fig. 4 is reasonably consistent with the model, there are, unfortunately, fewer measurements made in the attenuation phase that are also based on a single interaction with the sea surface, such as the measurements in Fig. 4. The measurements of Wille and Geyer [4] show convincingly, however, how an excess total transmission loss in shallow water involving both sea surface and seabed interaction, increases and becomes strongly dependent on wind speed, when in their case the wind speed exceeds about 10 m/s, and thus are somewhat consistent with Fig. 4. (In this case, one component of excess transmission loss is due to scattering into higher grazing angles with energy subsequently lost to the seabed.)

The field measurements reported in McConnell [11] represent intriguing observations apparently made under conditions of total occlusion, for which an energy loss bound is observed. These measurements (plotted on the far right side of Fig. 4) were also interleaved with measurements of vertical and horizontal spatial coherence, the results of which were first given in a 1990 report [12] and re-visited here. Figure 5 shows the estimates of horizontal and vertical coherence compared with model-bands for spatial coherence, computed using the method from [5]. The three versions of model-bands are based on rough-surface scattering equivalent to a wind speed of 17 m/s and fetch of 40 km, plus scattering and attenuation from bubbles for three cases: no bubbles, bubble concentration from Eq. (3) for wind speed of 10 m/s, and for wind speed of 17 m/s representing total occlusion. The model-bands incorporate uncertainties (the bands) in the six receiving beams involved in the measurements, three distributed horizontally and three vertically, and appear nominally consistent with the coherence estimates. (Here the apparent insensitivity of the models for vertical coherence to bubble concentration, is due to the individual beam patterns that compose the vertical receiving array.) Most significant, however, is that horizontal coherence must always exceed vertical coherence for sea surface forward scattering with this acquisition geometry, yet it can be seen in Fig. 5 that horizontal coherence has been knocked down to levels predicted by bistatic scattering from near-surface bubbles and subsequent total occlusion of the sea surface.

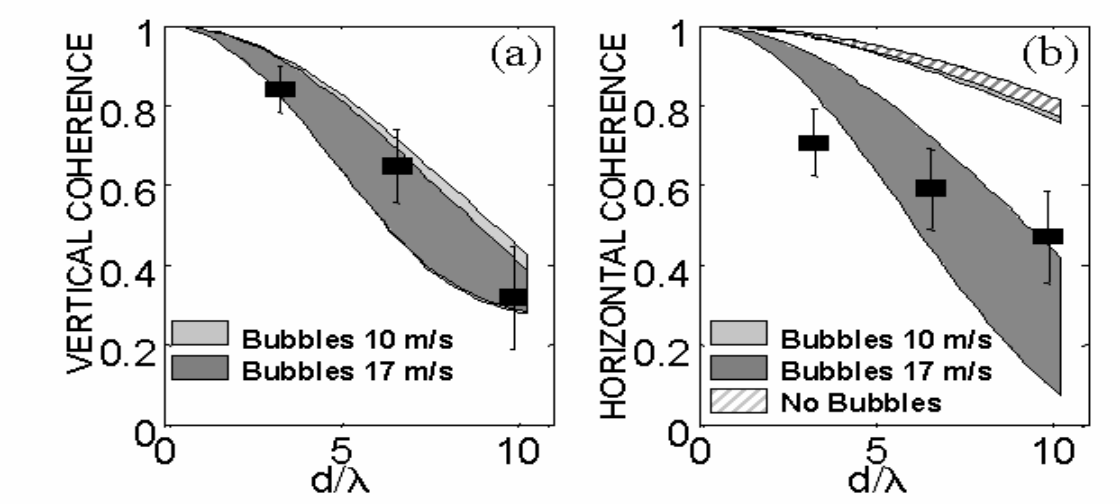

FIGURE 5. Estimates of the magnitude of vertical (a) and horizontal (b) spatial coherence plotted as a function of receiver separation normalized by 15-kHz wavelength. Model-bands are derived using rough-surface bistatic cross section at wind speed 17 m/s and three cases for bubbles: no bubbles, bubble concentration at 10 m/s, and 17 m/s. For vertical coherence the case of no bubbles and bubble concentration at a wind speed of 10 m/s are indistinguishable.

SUMMARY

A model for energy loss in the sea surface bounce path due to attenuation from near-surface bubbles has been presented; it applies to the nominal frequency range O(10–100) kHz and assumes the parameter c is >> 1. The model compares reasonably well with measurements from the recent ASIAEX experiment and archival data sets. Three phases of impact of bubbles on forward scattering from the sea surface are illustrated: the first is no discernable attenuation, which occurs under mild conditions (wind speed < 5–7 m/s), wherein bubbles extend the pulse forward scattered from the sea surface, but only at levels 30 dB below the peak level, which itself is not attenuated. The second occurs under more vigorous conditions (wind speed 7–12 m/s); here a real energy loss is observed, but time and angle spreading (dominated by rough surface scattering) remain relatively unchanged. The third occurs under still more vigorous conditions (wind speed > 12–15 m/s); here there is near total occlusion of the sea surface, time and angle spreading are manifestly altered, and bubble-mediated energy loss becomes bounded by scattering from bubbles. Although two major effects of total occlusion, the reduction in horizontal spatial coherence and the bounding of attenuation, were demonstrated with field data, additional field measurements of this phenomenon are needed to verify the model presented here.

ACKNOWLEDGMENTS

This work was funded by the Office of Naval Research, Ocean Acoustics Program.

REFERENCES

1. Dahl, P.H., "On Bistatic Sea Surface Scattering: Field Measurements and Modeling," *J. Acoust. Soc. Am.*, **105,** 2155-2169 (1999).
2. Nichols, R.H., and Senko, A., "Amplitude Fluctuations of Low-Frequency Underwater Acoustic Pulses Reflected from the Ocean Surface," *J. Acoust. Soc. Am.*, **55,** 550-554 (1974).
3. Weston, D. E., "On Losses due to Storm Bubbles in Ocean Sound Transmission," *J. Acoust. Soc. Am.*, **86,** 1546-1552 (1989).
4. Wille, P.C. and D. Geyer, "Simultaneous Measurements of Surface Generated Noise and Attenuation at the Fixed Shallow Water Range *NORDSEE*," in: *Proceedings Advanced Research Workshop on Natural Mechanisms of Surface Generated Noise in the Ocean*, June 1987, Lerici, Italy, pp. 295-308.
5. Dahl, P.H. "The van Cittert-Zernike Theorem and Forward Scattering from the Sea Surface," *J. Acoust. Soc. Am.*, **115**, 589-599 (2004).
6. McDonald, J. F. and Spindel, R.C., "Implications of Fresnel Corrections in a non-Gaussian Surface Scatter Channel," *J. Acoust. Soc. Am.*, **50,** 746-757 (1971).
7. Dahl, P.H. "High-frequency Forward Scattering from the Sea Surface: The Characteristic Scales of Time and Angle Spreading," *IEEE J. Ocean. Eng.*, **26**, 141-151 (2001).
8. Dahl, P.H. "The Contribution of Bubbles to High-Frequency Sea Surface Backscatter: A 24-h Time Series of Field Measurements," *J. Acoust. Soc. Am.*, **113**, 769-780 (2003).
9. Tappert, F. D., "Inhomogeneous Absorption and Geometric Acoustics", *J. Acoust. Soc. Am.*, **103,** 1282-1287 (1998).
10. Thorsos, E. I., "High Frequency Surface Forward Scattering Measurements," presented at the 108th meeting of the Acoustical Society of America, October 1984.
11. McConnell, S. O. "Acoustic Measurements of Bubble Densities at 15-50 kHz," in: *Proceedings Advanced Research Workshop on Natural Mechanisms of Surface Generated Noise in the Ocean*, June 1987, Lerici, Italy, pp. 237-253.
12. Dahl, P.H. and McConnell, S. O. "Measurements of Acoustic Spatial Coherence in a Near-Shore Environment," APL-UW TR 9016, August 1990.